Comprehensive transcriptome profiling of T-2 toxin-induced nephrotoxicity in mice

Guoquan Wu , Xuan Wu , Yige Wu , Yuping Wu , Hui Li * , Chongshan Dai *

Posted Date: 11 December 2023

doi: 10.20944/preprints202312.0727.v1

Keywords: T-2 toxin; nephrotoxicity; transcriptome; RNA-seq; differential expression gene.

Article

Comprehensive Transcriptome Profiling of T-2 Toxin-Induced Nephrotoxicity in Mice

Guoquan Wu [1], Xuan Wu [2,3], Yige Wu [1], Yuping Wu [4], Hui Li [2,*], Chongshan Dai [1,*]

[1] National Key Laboratory of Veterinary Public Health and Safety, College of Veterinary Medicine, China Agricultural University, Beijing 100193, China
[2] Beijing Key Laboratory of Diagnostic and Traceability Technologies for Food Poisoning, Beijing Center for Disease Prevention and Control, Beijing 100013, China
[3] School of Public Health, Capital Medical University, Beijing 100069, China
[4] College of Life Science and Basic Medicine, Center for Biotechnology Research, Xinxiang University, Xinxiang, Henan, 453003, China
* Correspondence: lihui@bjcdc.org (H.L.); daichongshan@cau.edu.cn (C.D.); Tel.: +8610-64407193 (H,L,)

Abstract: Trichothecene mycotoxin T-2 toxin is an important environmental pollutant and poses a global threat to human and animal health. T-2 toxin could induce nephrotoxicity, however, the precise molecular mechanism remains unclear. In this study, the mice were intraperitoneally administrated with a single dose of 2 mg/kg T-2 toxin. The kidney function and ultrastructural observation were also assessed and found T-2 toxin could cause kidney damage. Transmission electron microscopy showed a significant swelling and vacuolization of the mitochondria of renal cell. A total of 1122, 58, and 391 genes that were predominantly expressed in kidney tissues at 1 d, 3 d, and 7 d after T-2 toxin exposure, respectively. Early transcriptomic changes at 1 d after exposure were down-regulation of DEGs involved in the cell cycle, p53 signaling pathway, and cellular senescence, while up-regulation of DEGs referred to the ribosome pathway. The temporal variations in gene expression pattern in T-2 toxin exposure in mice kidney were presented and cellular metabolism was disturbed at the exposure recovery period with 7 d. In conclusion, this study, for the first time, provided a comprehensive comparative transcriptomic analysis of gene regulation in T-2 toxin exposure-induced nephrotoxicity at different temporal periods and explored the nephrotoxicity mechanism of T-2 toxin at the mRNA level.

Keywords: T-2 toxin; nephrotoxicity; transcriptome; RNA-seq; differential expression gene

1. Introduction

T-2 toxin (Figure 1) is the most toxic trichothecene mycotoxin produced by a variety of Fusarium species [1–3]. T-2 toxin was reported to mainly contaminates wheat, barley, corn, and other food crops and their products and are posing a great threat to human and animal health [4]. According to the Biomin Global Mycotoxin Report, the prevalence of T-2 toxin in agricultural products in global 75 countries has significantly increased from 23% in 2018 to 38% in 2020 [5]. Epidemiological studies demonstrate that T-2 toxin can be transmitted through food chain. Several studies also indicated that T-2 toxin exposure was an important pathogenesis factor for human fatal alimentary tract toxic Aleutian and Kashin Beck disease (KBD) [6,7]. Accumulating evidences suggest that T-2 toxin exerts various potential toxic effects, including immunotoxicity [8], nephrotoxicity [9–12], neurotoxicity [13,14], cardiotoxicity [15,16], and reproductive toxicity [17–19]. T-2 toxin has been recognized as an important environmental pollutant [20]. Therefore, to discover effective prevention and control strategies for T-2 toxin exposure, it is very necessary to explore its toxic molecular mechanisms.

Preprints (www.preprints.org) | NOT PEER-REVIEWED | Posted: 11 December 2023 doi:10.20944/preprints202312.0727.v1

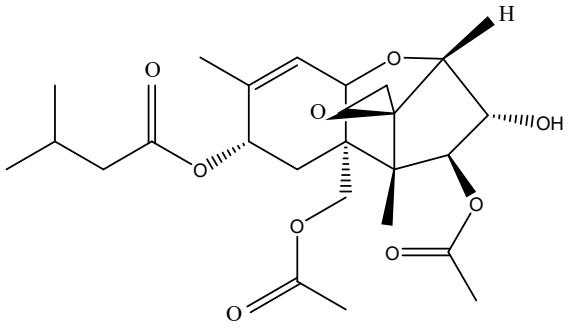

Figure 1. Chemical structure of T-2 toxin.

Recent studies have revealed that the kidney is one of the major target organs for T-2 toxin exposure [9,11,12]. It has been reported that T-2 toxin exposure could induce apoptotic cell death in kidney tissues of mice and renal cell lines, and kidney interstitial fibrosis in severe cases [10,11]. T-2 toxin could interact with cell membranes and enter the cell to bind to ribosomal subunits and inhibit protein synthesis [21–23]. A previous study also found that T-2 toxin exposure could trigger the production of reactive oxygen species (ROS), then inducing oxidative stress and inflammatory response, disruption of multiple metabolic pathways (i.e., energy and amino acids), ultimately resulting in structural and functional damage to the kidney. Several studies have reported that T-2 toxin can impair mitochondrial function by inhibiting the electron transport chain and attack the phospholipids in the cell membrane [3,18,24,25]. This would trigger mitochondrial apoptosis by the activation of various signaling mediators including MAPKs and caspases.

The signaling mediators are orchestrated and regulated by the cooperative and/or antagonistic actions of nuclear factor (NF-κB), HIF1α, the mechanistic target of rapamycin (mTOR), and the phosphatidylinositol 3-kinase (PI3K)/protein kinase B (AKT) signaling pathway. Currently, several studies have reported mitogen-activated protein kinase (MAPK), Wnt/β-catenin, EGFR, mTOR, and p53 were associated with renal fibrosis [7,10,11,18]. Existing evidence suggests that oxidative stress, apoptosis was correlated with the nephrotoxicity of T-2 toxin. The mechanism of action of T-2 toxin induced nephrotoxicity was complex and the comprehensive alternations of gene expression of T-2 toxin exposure and important functional gene biomarker have not been deeply addressed. Recently, the next-generation RNA-sequencing (RNA-seq) technology combined with advanced bioinformatics analysis has incited to explore the complexities of genetic information at a specific time and state. RNA-seq has been widely used in the progressively increasing demand for toxicity of mycotoxin and environmental pollutants.

In this study, we analyzed the transcriptomes of murine kidney tissue at different temporal phases to infer the molecular mechanism and potential biomarkers associated with T-2 toxin-induced nephrotoxicity. Our study will help to reveal the vital perturbation pathways of T-2 toxin-induced nephrotoxicity and enrich the insights into T-2-induced toxicity.

2. Materials and Methods

2.1. Chemicals and Reagents

T-2 toxin (CAS NO. 21259-20-1) (Purity ≥ 99%) was purchased from Sigma-Aldrich (St. Louis, MO, USA). Sodium dodecyl sulfonate (SDS), dimethyl sulfoxide (DMSO), and Tris hydroxymethyl (Tris-HCl) were purchased from AMRESCO Inc. (Solon, OH, USA). T-2 toxin was prepared in DMSO at a concentration of 10 μg/mL stock solution and stored at −20 °C.

2.2. Animals

Forty male wile-type (WT) C57BL/6N mice aged 4 weeks were obtained from Beijing Vital River Laboratory Animal Technology Co., Ltd (Beijing, China). The mice were housed at 22-24 ℃ and subjected to a 12 h/12 h light/dark cycle with 50%-60% humidity, and provided a standard pellet diet

 doi:10.20944/preprints202312.0727.v1

and drinking water ad libitum. No animal mortality occurred during the study period. The mice were randomly assigned to the control group (CG) and T-2 toxin treatment groups (TGs) (n = 5 per group). T-2 toxin was dissolved in DMSO and added in saline for dilution. The CG were administrated with 0.5%DMSO and the TGs were injected intraperitoneally with a single dose of 2 mg/kg T-2 toxin bodyweight (BW). The BW of mice was measured at the 1 d, 3 d, and 7 d after administration, and the dose was adjusted according to the BW. All animal experiments were approved by the Animal Care and Use Committee of China Agricultural University (Research license AW14010202-2-4) and performed according to the guidelines for animal experiments at China Agricultural University.

2.3. Tissue Sample Collection

Mice were humanely sacrificed and the kidney was quickly excised and quenched with liquid nitrogen and stored at -80 °C until analysis. We collected the mice kidney tissue samples at four time points: 0 d (before administration), and at 1, 3, and 7 d after intraperitoneal administration. The mouse kidney tissues were fixed with 10% ZnCl2 formalin solution before histopathological examination. The fixed organs were dehydrated in graded alcohol solutions, embedded in paraffin and 3-μm sections were cut and stained with H&E. The representative images were scanned using a slicing scanner and viewed using CaseViewer_2.0 software.

2.4. Biochemical Assay

The activities of serum urea (UREA), creatinine (CRE), and creatine kinase (CK) at different periods were measured with the kits supplied by Nanjing Jiancheng Bioengineering Institute (Nanjing, China) according to the manufacturer's instructions.

2.5. Ultrastructural Analysis of Kidney

Kidney ultrastructure was further analyzed using a standard transmission electron microscopy (TEM, H-7800, Hitachi, Japan). Fresh kidneys were fixed with 1% osmium tetroxide/1.25% potassium ferricyanide/0.15 M sodium phosphate buffer (pH 7.4) for 1 h, then rinsed three times with 0.15 M sodium phosphate buffer and washed with deionized water (pH 7.4). The kidneys were dehydrated twice with propylene oxide (15 min each time) and ethanol (30, 50, 75, and 100% for 10 min each time). The kidney was embedded in new propylene oxide/Polybed 812 epoxy resin, and then penetrated overnight (Polysciences, Warrington, PA).

2.6. RNA-Seq

Kidneys were maintained in tubes on dry ice and homogenized tissue was kept in tubes on ice prior to analysis. Total RNA was extracted from kidney tissues preserved in RNAlater solution by using Trizol reagent (Thermo Fisher Scientific). The aqueous phase of the Trizol extract was purified with the PureLinkTM RNA Mini Kit (Thermo Fisher Scientific) following the manufacturer's instructions. RNA was used for library construction employing the TruSeq Stranded mRNA LT Sample Prep Kit (Illumina, San Diego, CA) according to the manufacturer's protocol. RNA integrity was assessed using Agilent TapeStation 2200 System (Agilent Technologies, Santa Clara, CA). The libraries were sequenced on the BGISEQ-500 platform in combination with a tag-based digital gene expression system. The reads were aligned to the reference genome using TopHat [26] with the Refseq gene annotation. Expression levels (FPKM) of Refseq genes were calculated using Cufflinks [26]. Differentially expressed genes (DEGs) were identified using DESeq2 [27].

2.7. Statistical Analysis

For transcriptomics analysis, statistical significance was considered with adjusted $p < 0.01$ values and fold change ≥ 2 with n = 5 per group. We used Graphpad Prism 9.3 to analyze the data and the data is displayed as mean ± SD. The statistical analysis of the experimental data was performed using SPSS 20.0 (IBM SPSS, Inc., USA). One-way analysis of variance (ANOVA) was used to analyze the difference among groups. A p value < 0.05 was considered statistically significant.

 doi:10.20944/preprints202312.0727.v1

3. Results

3.1. T-2 Toxin Induced Kidney Damages

Trichothecenes cause growth retardation, hemorrhagic lesions, immune dysfunction, and vomiting, and are multi-organ toxic [3,28]. We analyzed the effects of T-2 toxin on BW and growth rate of the mice in the TG group (**Table S1**). The BW of the mice at 0 d in CG and TG were 20.76 and 20.65 g, respectively. The BW of the mice in CG and TG groups increased during the seven days experimental period, and the BW of mice in TG group grow slower than that in the CG group. The terminal BW of the mice in the TG group at 3 d and 7 d were 22.97 and 22.12 g, respectively, which were significantly higher than that of the CG at 0 d (before administration) ($p < 0.05$). We further analyzed the changes in BW of mice among the TG at different periods. The results showed that the BW of the mice at 3 d and 7 d was notably differ from that at the 0 d and 1 d ($p < 0.05$). By comparing the growth rate between 0 d and 7d, we found that T-2 toxin suppressed the growth of the mice with the growth rate of 9.56% and 7.19% in TG and CG, respectively.

We found slight swelling of renal tubular epithelial cells with scattered distribution of tubular hyaline tubular patterns based on the histological analysis (Figure 2A–D). It indicates that T-2 toxin exclusively causes damage to the kidney. Furthermore, we assessed the integrity and dysfunction of kidney cells using classic biomarkers (e.g. UREA, CRE, and CK). Intriguingly, three important kidney biochemical index (UREA and CRE) in TG groups exhibited the decrease trend at 1 d and 3 d compared with the CG group. The serum levels of UREA at 3 d in CG group were significantly increased than those at 1 d after T-2 toxin administration ($p < 0.05$), and indicated that the kidney damages occurred in the toxin exposure period. For CRE, its serum levels at 7 d were significantly higher than those at 3 d in TG groups ($p < 0.05$). However, the levels of CK did not change significantly in the different treatment groups (Figure 3).

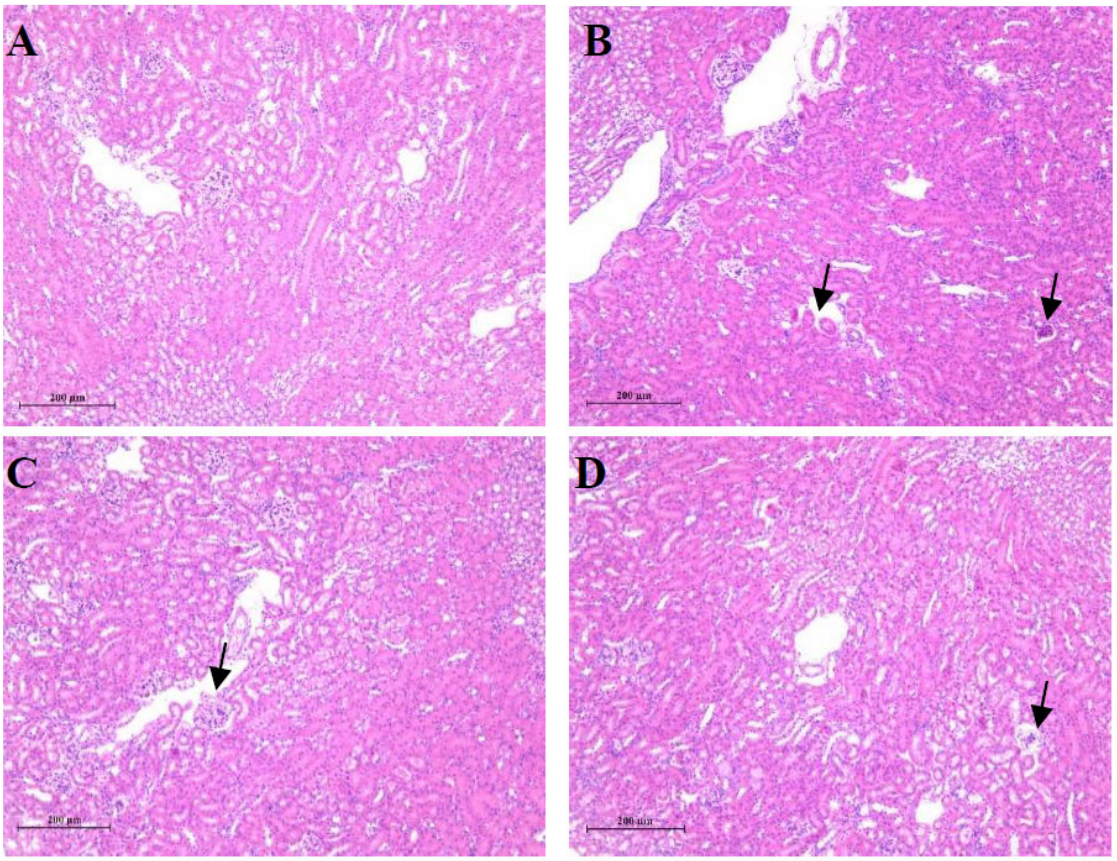

Figure 2. T-2 toxin induced kidney damage in mice. Black arrows represent slight swelling of renal tubular epithelial cells. Mice was intraperitoneally administrated with T-2 toxin at a single dose of 2

Preprints (www.preprints.org) | NOT PEER-REVIEWED | Posted: 11 December 2023 doi:10.20944/preprints202312.0727.v1

mg/kg body weight (n = 5 for mice). Representative H&E images of kidney in CG and TG mice at 0 d (before administration, **A**), 1 d (**B**), 3 d (**C**), and 7d (**D**).

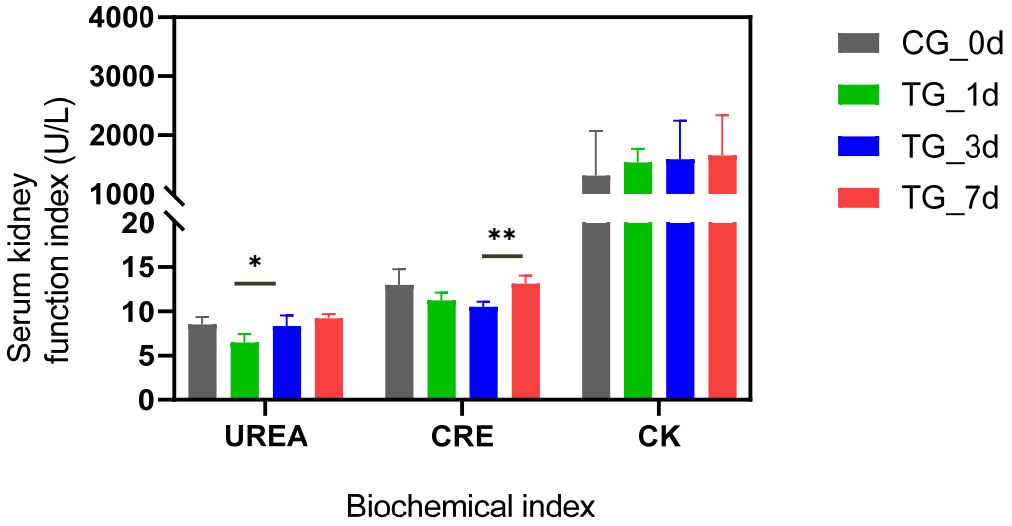

Figure 3. Serum levels of kidney biomarkers including UREA, CRE, and CK in mice on plasma. Data were shown as mean ± SD.

3.2. T-2 Toxin-Induced Kidney Ultrastructural Changes

We performed electron microscopical analysis and found a significant swelling and vacuolization of the mitochondria (Figure 4). Ultrastructural changes such as nuclear chromatin condensation and side shift in the epithelial nucleus of proximal tubule, cellular mitochondrial swelling, cavitation, or epithelial degeneration, and lysosomal increase in epithelial cells were shown (Figure 4).

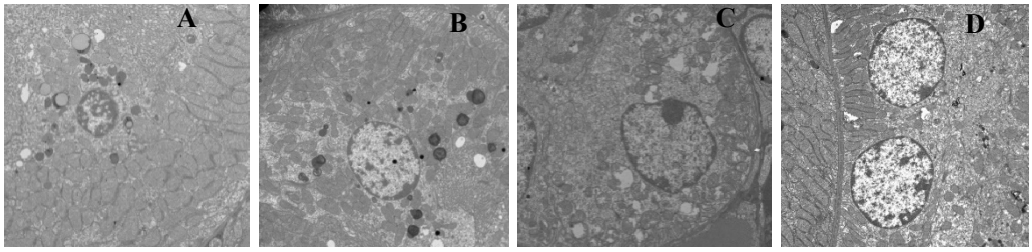

Figure 4. Representative TEM images of mice kidneys before (0 d, **A**) and after (1 d, **B**; 3 d, **C**, and 7 d, **D**) T-2 toxin exposure (magnification, 20,000×).

3.3. Transcriptome Analysis of Kidney Injury Induced by T-2 Toxin

We collected mice kidney tissues at 1 d, 3 d, and 7 d after T-2 toxin exposure and performed RNA-seq. Each sample produced an average of 1.18 G of data. The raw data from sequencing contained low-quality, junction-contaminated, and high unknown base N reads, which needed to be removed prior to data analysis to ensure the reliability of the results. Then we utilized the reference genome (GCF_000001635.26_GRCm38.p6) of mice (species: Mus_musculus) in the NCBI database for functional annotation. A total of 97,608 mRNA, 103,339 IncRNA, and 1,976 miRNA were found in this study. The average comparison rate of the samples against the gene set was 96.62% and the average comparison rate against the gene set was 62.73% (Table S2). A total of 19,513 genes were detected. Volcano plots for comparison of gene expression patten between TG_1d, TG_3d, and TG_7d were shown in Figure 5A–C. The fragments per kilobase per million (FPKM) > 10 with fold change > 2 and adjusted $p < 0.01$ were filtered to screen the candidate DEGs. We identified a total of 1122, 58,

Preprints (www.preprints.org) | NOT PEER-REVIEWED | Posted: 11 December 2023 doi:10.20944/preprints202312.0727.v1

and 391 genes that were predominantly expressed in kidney tissues at 1d, 3d, and 7d after T-2 toxin exposure, respectively (Figure 5D). A total of seven genes (Hba-a2, Alas2, Kif20a, Mup3, Ugt2b35, Mmp12, and Myh4) were distributed in all the three TG groups. We then compared the expression of the DEGs between three different groups and most DEGs were up-regulated at TG_1d and TG_7d (Figure 5E).

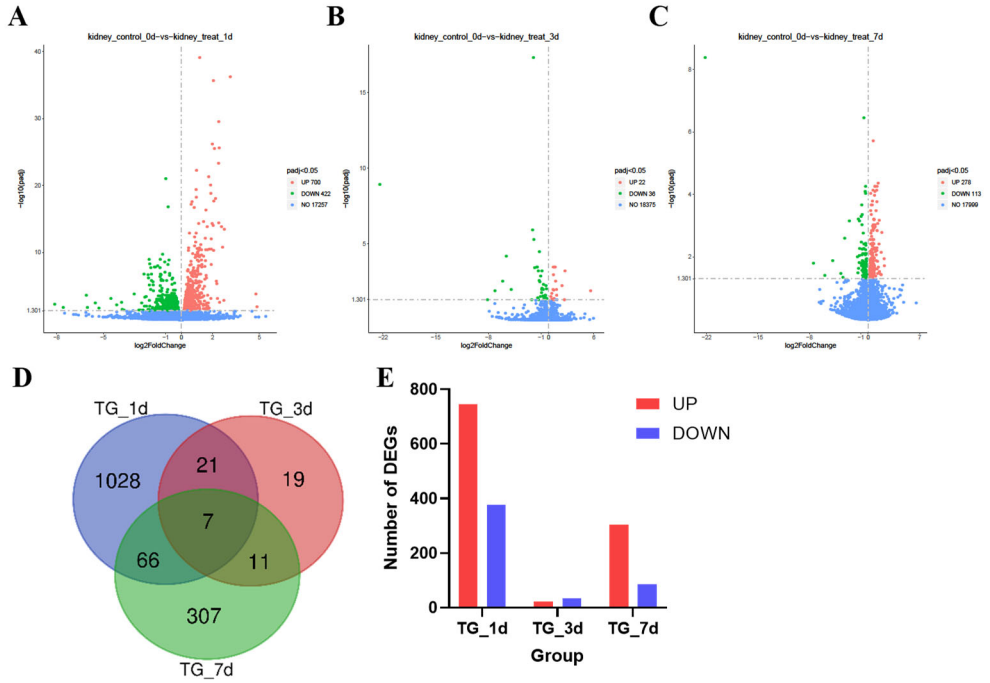

Figure 5. Transcriptome profiling of T-2 toxin-induced nephrotoxicity in mice. Volcano plots for comparison of gene expression patten between TG_1d (**A**), TG_3d (**B**), and TG_7d (**C**). (**D**) Venn diagram of DEGs in each group. (**E**) The number of the up-regulated and down-regulated DEGs in each group.

Next, we performed transcriptome profiling of mice kidney at 1d after T-2 toxin exposure. GO function enrichment analysis indicated that the DEGs were mainly enriched in cellular process, metabolic process, biological regulation, regulation of biological process, response to stimulus, etc (Figure 6A). We conducted functional annotation of the gene lists using ConsensusPathDB [29]. Intriguingly, the top-ranked pathway related to the cell cycle, p53 signaling pathway, and cellular senescence were over-presented in the TG_1d gene list. The top pathway including ribosome, proteasome, protein processing in endoplasmic reticulum, antigen processing and presentation, steroid biosynthesis, fatty acid elongation, alanine, aspartate and glutamate metabolism, terpenoid backbone biosynthesis, fatty acid degradation, measles, and circadian rhythm were overexpressed at 1 d after T-2 toxin exposure (Figure 6B). Kegg pathway enrichment results showed that the DEGs induced by T-2 toxin were enriched in AMPK signaling pathway, FoxO signaling pathway, NOD-like receptor signaling pathway, and metabolic pathways (Figure 6B). We found that the key seven genes including Bnip3, Tnfsf10, Ccnd1, Pten, Pck1, Sgk2, Prkag3 were involved in FoxO signaling pathway. A total of 44 ribosome related genes (e.g. Rps7, Rps21, Rpl4, Rps3a1, Rps2, etc) were over-presented after T-2 toxin exposure. Protein processing in endoplasmic reticulum including Eif2ak2, Hsp90b1, Hspa5, Lman1, Dnaja1, Svip, Hsp90ab1, and Hspbp1 was also disturbed in this exposure period. Some genes important for the AMPK signaling pathway (Fbp2, Eef2, Ppargc1a, Ccnd1, Eif4ebp1, Pck1, Ppp2r5a, Prkag3, and Pfkp genes) were also up-regulated in this acute T-2 toxin exposure.

Preprints (www.preprints.org) | NOT PEER-REVIEWED | Posted: 11 December 2023 doi:10.20944/preprints202312.0727.v1

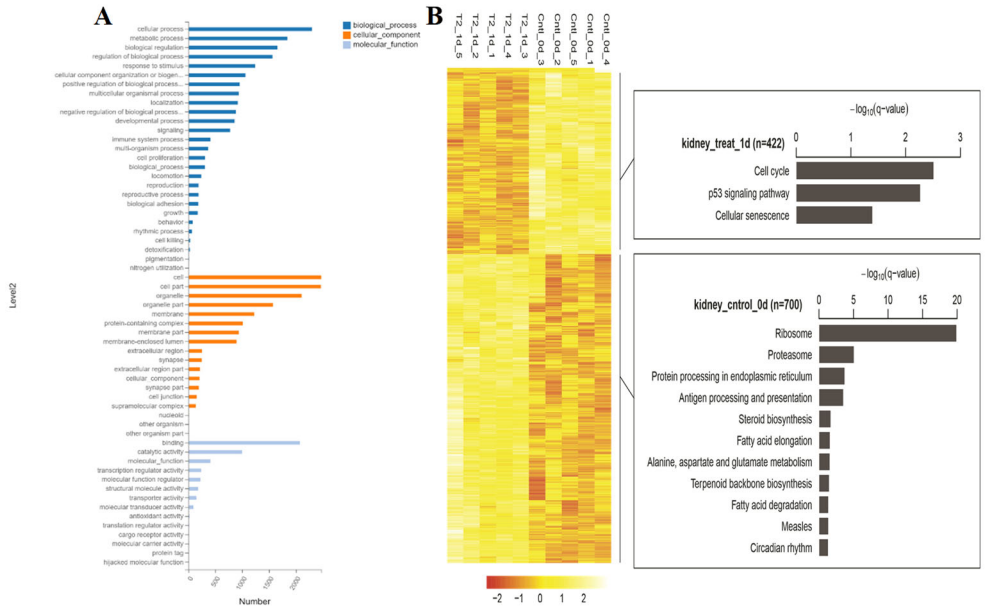

Figure 6. Transcriptome profiling of mice kidney at 1 d after T-2 toxin exposure. (**A**) GO functional enrichment of DEGs in TG_1d group. The horizontal coordinate is the number of DEGs and the vertical coordinate is the categorical entry of GO. (**B**) Heatmap representation of Z score-transformed FPKM of genes predominantly expressed in TG_1d group (left). The genes are ranked in descending order according to their FPKM. Overrepresented pathways are shown on the right. The top ranked pathways are shown with q-values.

GO analysis demonstrated that regulation of APC/C activators between G1/S and early anaphase, response to stilbenoid, regulation of cell cycle process, porphyrin metabolism, regulation of transferase activity, and MAPK cascade (Figure S1A). Consistently, the top-ranked pathway for the T-2_3d group was cell cycle, p53 signaling pathway, and cellular senescence for the upregulated DEGs (Figure S1A). Porphyrin metabolism, pentose and glucuronate interconversions, ascorbate and aldarate metabolism, chemical carcinogenesis - DNA adducts, drug metabolism, and retinol metabolism were significant pathway for the downregulated DEGs (Figure S1B). Two genes Ccna2 and Slc2a4 were important for the AMPK signaling pathway and FoxO signaling pathway. Four genes (Ccna2, Cdc20, Ccnb1, and Cdk1) were involved in the cell cycle pathway to modulate the repair of the T-2 toxin induced nephrotoxicity (Figure S2). For Wnt signaling pathway, we found that Frzb and Sfrp1 were involved in this exposure period. Importantly, p53 signaling pathway was affected by disturbing the expression of Ccnb1, Rrm2, and Cdk1genes. Porphyrin metabolism was over-expressed and Ugt2b35, Alas2, and Ugt2a2 genes were affected in this process. We also found that Reln gene was involved in the PI3K-Akt signaling pathway.

We further characterize the transcriptomic profile of T-2 toxin exposure at 7 d and the number of the DEGs was increased approximately 6.74-fold change compared with that at 3 d (Figure 5D). Notably, most genes were upregulated in this exposure period (Figure 5E). We speculated the mice might have a process of self-repairing protection, and this protection may be only temporary after acute exposure to T-2 toxin. GO analysis found that monocarboxylic acid metabolic process, metabolism of lipids, biological oxidations, steroid metabolic process, protein localization, metabolism of xenobiotics by cytochrome P450, PPAR signaling pathway, and mitochondrial long chain fatty acid beta oxidation were enriched using Metascape software (Figure S3A). Kegg pathway analysis showed that peroxisome, porphyrin metabolism, PPAR signaling pathway, fatty acid degradation, butanoate metabolism, steroid hormone biosynthesis, ferroptosis and fatty acid metabolism were over-presented in T-2 toxin exposure (Figure S3B). Slc3a2, Slc39a8, Map1lc3a, Hmox1, Gpx4, and Fth1were associated with ferroptosis pathway. MAPK signaling pathway was disturbed by regulating the expression of Cd36, Hmgcr, Ccnd1, Pck1, Pfkfb2, and Scd2 (Figure S4).

Preprints (www.preprints.org) | NOT PEER-REVIEWED | Posted: 11 December 2023 doi:10.20944/preprints202312.0727.v1

3.4. Temporal Pattern and Network Analysis of Transcriptional Regulators

We identified the transcriptional regulators likely to be involved in the mice kidney after T-2 toxin exposure at three different time points. Activated regulators, such as Irf1, Cebpb, Nr3c1, Trp53, Nfkb1, Spic, Egr1, Foxo4, Ep300, Clock, and Stat1 may play important roles for T-2 toxin exposure at 1 d (Figure S5A). On the other hand, at 3 d after exposure, Trp53 was important regulating genes involved in autophagy (Figure S5B). There are two important regulatory gene Ppara and Bcl3 that are predicted to be activated in 7 d after T-2 toxin exposure (Figure S5C). Molecular network analysis revealed that the DEGs (Rpl8, Rps15a, Rpl19, Rpl11, Rps18, Rps5, Rpl5, Rpl0, Rack1, and Rps3) were mainly involved in Ribosome-related pathway at 1 d after T-2 toxin exposure (Figure 7A). At 3d after exposure, the key regulators including Cdc20, Top2a, Cona2, Ube2c, Kif20a, Prc1, Aspm, Mki67, Rrm2, and Cdk1 were referred to Cell cycle, cellular senescence, ubiquitin mediated proteolysis, and p53 signaling pathway (Figure 7B). Notably, Cyp2e1, Cyp4a14, Ugt2b34, Ugt2b37, Ugt2b35, Ugt2b38, and Cyp2a4 were the important regulators and mainly involved in cellular metabolism at the exposure recovery period (Figure 7C).

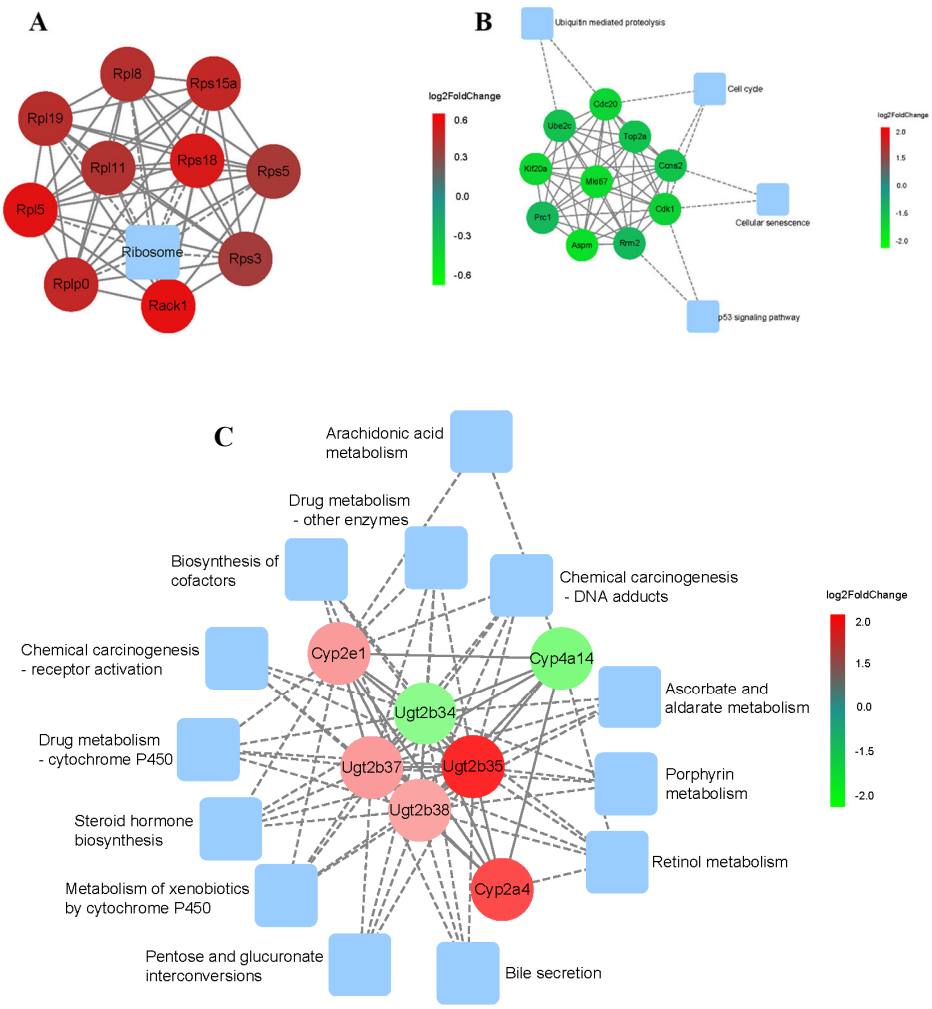

Figure 7. Mechanism networks of transcriptomic regulators and their relationship by Cytoscape. (**A**) Network analysis of DEGs at 1 d. (**B**) Network analysis of DEGs at 3 d. (**C**) Network analysis of DEGs at 7 d.

4. Discussion

Trichothecene mycotoxins are a worldwide priority for in food safety and environmental exposure. T-2 toxin is one of the most common and toxic trichothecene mycotoxins. Previous studies have shown that trichothecenes inhibited mitochondrial translation prior to depolarization and

 doi:10.20944/preprints202312.0727.v1

fragmentation of the mitochondrial membrane and were not associated with the cellar translation inhibition [30,31]. The induction of reactive oxygen species (ROS) levels and oxidative stress, thereby disrupting the activity or the production of antioxidant enzymes is considered an important mechanism of toxicity of T-2 toxins [32]. However, the in-depth mechanism of toxicity of T-2 toxin exposure is poorly understood. To obtain a comprehensive view of the cellular transcriptome characterization of T-2 toxin exposure, we performed next-generation RNA-seq approach to delineate T-2 toxin induced nephrotoxicity at different temporal exposure (1 d, 3 d, and 7 d).

Our data revealed that different transcriptomic profiling of mice kidney was presented at three time points. There are marked differences during the three different exposure period. Transcriptomic changes were exhibited at 1 d after exposure and important marker genes included 27 ribosome associated genes (Rps7, Rps21, Rpl4, Rps3a1, Rps2, Rpl3, Rps26, Rpl19, Rps27l, Rpl30, Rps13, Rplp2, Rpl27, Rpl13, Rpsa, Rpl7a, Rps3, Rps5, Mrpl18, Rplp0, Rpl24, Rpl5, Rpl9, Rpl29, Rps15a, Rps4x, and Mrps10), 14 proteasome (Psme2, Psmd12, Psma1, Psmc4, Psmc6, Psmd4, Psmb2, Psme1, Psma6, Psmb8, Psmd8, Psmc3, Psmb10, and Psmc1), 12 protein processing in endoplasmic reticulum (Selenos, Eif2ak2, Hsp90b1, Hspa5, Lman, Dnaja1, Svip, Hsp90ab1, Hspbp1, Derl3, Rad23a, and Ero1lb) (Figure 6). Notably, all 27 DEGs in the Ribosome pathway encode ribosomal proteins and show an up-regulation trend. Previous studies revealed that T-2 toxin could inhibit protein synthesis in eukaryotic cells [33]. Most strikingly, FoxO signaling pathway might be dispensable for the kidney damage. FoxO signaling pathway are required for regulating various biological activities such as proliferation, apoptosis, migration, and oxidative stress [34]. FoxO-dependent gene expression profiles are specific to cell types and stimuli, and unique combinations of environmental signals trigger transcriptional programs that promote cell cycle arrest and survival in response to stress or induction of apoptosis [34]. Yang et al. demonstrated that IL 6 and FoxO3 were enriched in the FoxO signaling pathway and involved in the expression profiles of selenium-related genes in human chondrocytes after exposure to T-2 toxin [35].

The transcription factor networks may also be different during the three different exposure periods. We found that some key transcription factors regulated the expression in kidney tissue. Cell cycle genes included Ccna2, Cdc20, Ccnb1, and Cdk1were be affected at 3 d after T-2 toxin exposure (Figure S2). In addition, p53 signaling pathway was identified upon T-2 toxin exposure. The p53 signaling pathway can be activated by stress signals, such as oxidative stress and DNA damage, and involves activation of cell apoptosis [36]. Recently, Yu et al reported that T-2 toxin induces mitochondrial dysfunction in chondrocytes via the p53-cyclophilin D pathway and p53 played an important role in T-2 toxin-induced mitochondrial dysfunction [37]. Gene expression profile sequencing of human chondrocytes treated with T-2 toxin showed the p53 pathway was significantly expressed [35], which was consistent with our results.

5. Conclusions

Our study used advanced RNA-seq techniques to explore the comprehensive transcriptome profile of T-2 toxin induced nephrotoxicity in mice model and characterize gene expression during different exposure periods. T-2 toxin exposure can induce kidney damages and side shift in the epithelial nucleus of proximal tubule and cellular mitochondrial swelling. The temporal variations in gene expression pattern in T-2 toxin exposure in mice kidney were presented. Molecular signatures and signaling pathways specific to each exposure period were identified and ribosome pathway was overexpressed at the early exposure and cellular metabolism was disturbed at the exposure recovery period. Further study is warranted to decipher the role of key metabolism regulators of kidney damage in T-2 toxin induced nephrotoxicity.

Supplementary Materials: The following supporting information can be downloaded at online. Figure S1: Transcriptome profiling of mice kidney at 3 d after T-2 toxin exposure. Figure S2: Sankey diagram of KEGG pathway from overrepresentation analysis based on overlapping up-regulated and down-regulated genes in mice kidney at 3d after T-2 toxin exposure. Figure S3: Transcriptome profiling of mice kidney at 7 d after T-2 toxin exposure. Figure S4: Sankey diagram of KEGG pathway from overrepresentation analysis based on

overlapping up-regulated and down-regulated genes in mice kidney at 7 d after T-2 toxin exposure. Figure S5 Enrichment analysis of transcriptional regulators involved in T-2 toxin exposure at 1 d (A), 3 d (B) and 7d (C).

Author Contributions: Conceptualization, H.L. and C.S.D.; methodology, G.Q.W., H.L., C.S.D.; software, G.Q.W., Y.G.W., X.W.; validation, C.S.D.; formal analysis, G.Q.W., Y.P.W. and H.L.; investigation, G.Q.W., H.L., Y.P.W. and X.W.; resources, H.L.; data curation, H.L., C.S.D., G.Q.W. and Y.G.W.; writing—original draft preparation, G.Q.W.; writing—review and editing, H.L. and C.S.D.; visualization, H.L. and Y.P.W.; supervision, H.L. and C.S.D. All authors have read and agreed to the published version of the manuscript.

Data Availability Statement: Raw data are made available on request to the corresponding author.

Funding: This research was funded by the National Key Research and Development of China (Grant No. 2023YFF0613400).

Conflicts of Interest: The authors declare no conflict of interest.

References

1. Li, Y.; Wang, Z.; Beier, R.C.; Shen, J.; De Smet, D.; De Saeger, S.; Zhang, S. T-2 toxin, a trichothecene mycotoxin: review of toxicity, metabolism, and analytical methods. J Agric Food Chem 2011, 59, 3441-3453, doi:10.1021/jf200767q.
2. Marin, S.; Ramos, A.J.; Cano-Sancho, G.; Sanchis, V. Mycotoxins: occurrence, toxicology, and exposure assessment. Food Chem Toxicol 2013, 60, 218-237, doi:10.1016/j.fct.2013.07.047.
3. Bin-Umer, M.A.; McLaughlin, J.E.; Butterly, M.S.; McCormick, S.; Tumer, N.E. Elimination of damaged mitochondria through mitophagy reduces mitochondrial oxidative stress and increases tolerance to trichothecenes. Proc Natl Acad Sci U S A 2014, 111, 11798-11803, doi:10.1073/pnas.1403145111.
4. Polak-Sliwinska, M.; Paszczyk, B. Trichothecenes in Food and Feed, Relevance to Human and Animal Health and Methods of Detection: A Systematic Review. Molecules 2021, 26, doi:10.3390/molecules26020454.
5. Wang, J.X.; Zhao, Y.; Chen, M.S.; Zhang, H.; Cui, J.G.; Li, J.L. Heme-oxygenase-1 as a target for phthalate-induced cardiomyocytes ferroptosis. Environ Pollut 2023, 317, 120717, doi:10.1016/j.envpol.2022.120717.
6. Yan, D.; Kang, P.; Yang, J.; Shen, B.; Zhou, Z.; Duan, L.; Deng, J.; Huang, H.; Pei, F.X. The effect of Kashin-Beck disease-affected feed and T-2 toxin on the bone development of Wistar rats. Int J Rheum Dis 2010, 13, 266-272, doi:10.1111/j.1756-185X.2010.01530.x.
7. Xiao, B.; Wang, G.; Huo, H.; Li, W. Identification of HIF-1alpha/VEGFA signaling pathway and transcription factors in Kashin-Beck disease by integrated bioinformatics analysis. Exp Ther Med 2021, 22, 1115, doi:10.3892/etm.2021.10549.
8. Wu, Q.; Qin, Z.; Kuca, K.; You, L.; Zhao, Y.; Liu, A.; Musilek, K.; Chrienova, Z.; Nepovimova, E.; Oleksak, P., et al. An update on T-2 toxin and its modified forms: metabolism, immunotoxicity mechanism, and human exposure assessment. Arch Toxicol 2020, 94, 3645-3669, doi:10.1007/s00204-020-02899-9.
9. Zhang, X.; Wang, Y.; Yang, X.; Liu, M.; Huang, W.; Zhang, J.; Song, M.; Shao, B.; Li, Y. The nephrotoxicity of T-2 toxin in mice caused by oxidative stress-mediated apoptosis is related to Nrf2 pathway. Food Chem Toxicol 2021, 149, 112027, doi:10.1016/j.fct.2021.112027.
10. Zhang, X.; Li, B.; Huo, S.; Du, J.; Zhang, J.; Song, M.; Cui, Y.; Li, Y. T-2 Toxin Induces Kidney Fibrosis via the mtROS-NLRP3-Wnt/beta-Catenin Axis. J Agric Food Chem 2022, 70, 13765-13777, doi:10.1021/acs.jafc.2c05816.
11. Zhang, X.; Du, J.; Li, B.; Huo, S.; Zhang, J.; Cui, Y.; Song, M.; Shao, B.; Li, Y. PINK1/Parkin-mediated mitophagy mitigates T-2 toxin-induced nephrotoxicity. Food Chem Toxicol 2022, 164, 113078, doi:10.1016/j.fct.2022.113078.
12. Hou, L.; Liu, S.; Zhao, C.; Fan, L.; Hu, H.; Yin, S. The combination of T-2 toxin and acrylamide synergistically induces hepatotoxicity and nephrotoxicity via the activation of oxidative stress and the mitochondrial pathway. Toxicon 2021, 189, 65-72, doi:10.1016/j.toxicon.2020.11.007.
13. Dai, C.; Xiao, X.; Sun, F.; Zhang, Y.; Hoyer, D.; Shen, J.; Tang, S.; Velkov, T. T-2 toxin neurotoxicity: role of oxidative stress and mitochondrial dysfunction. Arch Toxicol 2019, 93, 3041-3056, doi:10.1007/s00204-019-02577-5.
14. Chaudhary, M.; Rao, P.V. Brain oxidative stress after dermal and subcutaneous exposure of T-2 toxin in mice. Food Chem Toxicol 2010, 48, 3436-3442, doi:10.1016/j.fct.2010.09.018.

15. Wang, C.; He, J.; Jin, H.; Xiao, H.; Peng, S.; Xie, J.; Zhang, L.; Guo, J. T-2 toxin induces cardiotoxicity by activating ferroptosis and inhibiting heme oxygenase-1. Chemosphere 2023, 341, 140087, doi:10.1016/j.chemosphere.2023.140087.
16. Dai, C.; Das Gupta, S.; Wang, Z.; Jiang, H.; Velkov, T.; Shen, J. T-2 toxin and its cardiotoxicity: New insights on the molecular mechanisms and therapeutic implications. Food Chem Toxicol 2022, 167, 113262, doi:10.1016/j.fct.2022.113262.
17. Yang, X.; Zhang, X.; Zhang, J.; Ji, Q.; Huang, W.; Zhang, X.; Li, Y. Spermatogenesis disorder caused by T-2 toxin is associated with germ cell apoptosis mediated by oxidative stress. Environ Pollut 2019, 251, 372-379, doi:10.1016/j.envpol.2019.05.023.
18. Lee, W.Y.; Park, H.J. T-2 mycotoxin Induces male germ cell apoptosis by ROS-mediated JNK/p38 MAPK pathway. Ecotoxicol Environ Saf 2023, 262, 115323, doi:10.1016/j.ecoenv.2023.115323.
19. Yang, X.; Liu, P.; Cui, Y.; Xiao, B.; Liu, M.; Song, M.; Huang, W.; Li, Y. Review of the Reproductive Toxicity of T-2 Toxin. J Agric Food Chem 2020, 68, 727-734, doi:10.1021/acs.jafc.9b07880.
20. Jacevic, V.; Wu, Q.; Nepovimova, E.; Kuca, K. Efficacy of methylprednisolone on T-2 toxin-induced cardiotoxicity in vivo: A pathohistological study. Environ Toxicol Pharmacol 2019, 71, 103221, doi:10.1016/j.etap.2019.103221.
21. Yu, X.; Zhang, C.; Chen, K.; Liu, Y.; Deng, Y.; Liu, W.; Zhang, D.; Jiang, G.; Li, X.; Giri, S.S., et al. Dietary T-2 toxin induces transcriptomic changes in hepatopancreas of Chinese mitten crab (Eriocheir sinensis) via nutrition metabolism and apoptosis-related pathways. Ecotoxicol Environ Saf 2023, 249, 114397, doi:10.1016/j.ecoenv.2022.114397.
22. Middlebrook, J.L.; Leatherman, D.L. Binding of T-2 toxin to eukaryotic cell ribosomes.
23. Li, J.; Wang, Y.; Deng, Y.; Wang, X.; Wu, W.; Nepovimova, E.; Wu, Q.; Kuca, K. Toxic mechanisms of the trichothecenes T-2 toxin and deoxynivalenol on protein synthesis. Food Chem Toxicol 2022, 164, 113044, doi:10.1016/j.fct.2022.113044.
24. Zhang, X.; Wang, Q.; Zhang, J.; Song, M.; Shao, B.; Han, Y.; Yang, X.; Li, Y. The Protective Effect of Selenium on T-2-Induced Nephrotoxicity Is Related to the Inhibition of ROS-Mediated Apoptosis in Mice Kidney. Biol Trace Elem Res 2022, 200, 206-216, doi:10.1007/s12011-021-02614-4.
25. Zhou, Y.J.; Zhang, S.P.; Liu, C.W.; Cai, Y.Q. The protection of selenium on ROS mediated-apoptosis by mitochondria dysfunction in cadmium-induced LLC-PK(1) cells. Toxicol In Vitro 2009, 23, 288-294, doi:10.1016/j.tiv.2008.12.009.
26. Trapnell, C.; Roberts, A.; Goff, L.; Pertea, G.; Kim, D.; Kelley, D.R.; Pimentel, H.; Salzberg, S.L.; Rinn, J.L.; Pachter, L. Differential gene and transcript expression analysis of RNA-seq experiments with TopHat and Cufflinks. Nat Protoc 2012, 7, 562-578, doi:10.1038/nprot.2012.016.
27. Love, M.I.; Huber, W.; Anders, S. Moderated estimation of fold change and dispersion for RNA-seq data with DESeq2. Genome Biol 2014, 15, 550, doi:10.1186/s13059-014-0550-8.
28. Meneely, J.; Greer, B.; Kolawole, O.; Elliott, C. T-2 and HT-2 Toxins: Toxicity, Occurrence and Analysis: A Review. Toxins (Basel) 2023, 15, doi:10.3390/toxins15080481.
29. Herwig, R.; Hardt, C.; Lienhard, M.; Kamburov, A. Analyzing and interpreting genome data at the network level with ConsensusPathDB. Nat Protoc 2016, 11, 1889-1907, doi:10.1038/nprot.2016.117.
30. Mclaughlin, J.E.; Bin-Umer, M.A.; Tortora, A.; Mendez, N.; McCormick, S.; Tumer, N.E. A genome-wide screen in Saccharomyces cerevisiae reveals a critical role for the mitochondria in the toxicity of a trichothecene mycotoxin. Proc Natl Acad Sci U S A 2009, 106, 21883-21888.
31. Bin-Umer, M.A.; McLaughlin, J.E.; Basu, D.; McCormick, S.; Tumer, N.E. Trichothecene mycotoxins inhibit mitochondrial translation--implication for the mechanism of toxicity. Toxins (Basel) 2011, 3, 1484-1501, doi:10.3390/toxins3121484.
32. Wu, Q.H.; Wang, X.; Yang, W.; Nüssler, A.K.; Xiong, L.Y.; Kuča, K.; Dohnal, V.; Zhang, X.J.; Yuan, Z.H. Oxidative stress-mediated cytotoxicity and metabolism of T-2 toxin and deoxynivalenol in animals and humans: an update. Arch Toxicol 2014, 88, 1309-26. doi: 10.1007/s00204-014-1280-0.
33. Cundliffe, E.; Cannon, M.; Davies, J. Mechanism of inhibition of eukaryotic protein synthesis by trichothecene fungal toxins. Proc Natl Acad Sci U S A 1974, 71, 30-34.
34. Charitou, P.; Burgering, B.M. Forkhead box(O) in control of reactive oxygen species and genomic stability to ensure healthy lifespan. Antioxid Redox Signal 2013,19, 1400-1419. doi: 10.1089/ars.2012.4921.

35. Yang, L.; Zhang, J.; Li, X.; Xu, C.; Wang, X.; Guo, X. Expression Profiles of Selenium-Related Genes in Human Chondrocytes Exposed to T-2 Toxin and Deoxynivalenol. Biol Trace Elem Res 2019, 190, 295-302, doi:10.1007/s12011-018-1560-2.
36. Yang, G.; Zhou, X.; Wang, J.; Zhang, W.; Zheng, H.; Lu, W.; Yuan, J. MEHP-induced oxidative DNA damage and apoptosis in HepG2 cells correlates with p53-mediated mitochondria-dependent signaling pathway. Food Chem Toxicol 2012, 50, 2424-2431, doi:10.1016/j.fct.2012.04.023.
37. Yu, F.F.; Yu, S.Y.; Sun, L.; Zuo, J.; Luo, K.T.; Wang, M.; Fu, X.L.; Zhang, F.; Huang, H.; Zhou, G.Y., et al. T-2 toxin induces mitochondrial dysfunction in chondrocytes via the p53-cyclophilin D pathway. J Hazard Mater 2023, 465, 133090, doi:10.1016/j.jhazmat.2023.133090.